IR WINDOW STUDIES

Ferdinand Kroger, et al

University of Southern California

Prepared for:

Air Force Cambridge Research Laboratories

15 March 1973

AFCRL-TR-73-0325

USCEE Report 454

UNIVERSITY OF SOUTHERN CALIFORNIA

IR WINDOW STUDIES

F. A. Krüger and John H. Marburger

Contract No. F19628-72-C-0275

Quarterly Technical Report No. 3
15 March 1973

Contract Monitor: Alfred Kahan
Solid State Sciences Laboratory

Approved for public release; distribution unlimited.

Prepared for the Defense Advanced Research Projects Agency

ARPA Order No. 2055, as Monitored by

AIR FORCE CAMBRIDGE RESEARCH LABORATORIES
AIR FORCE SYSTEMS COMMAND
UNITED STATES AIR FORCE
BEDFORD, MASSACHUSETTS 01730

ELECTRONIC SCIENCES LABORATORY

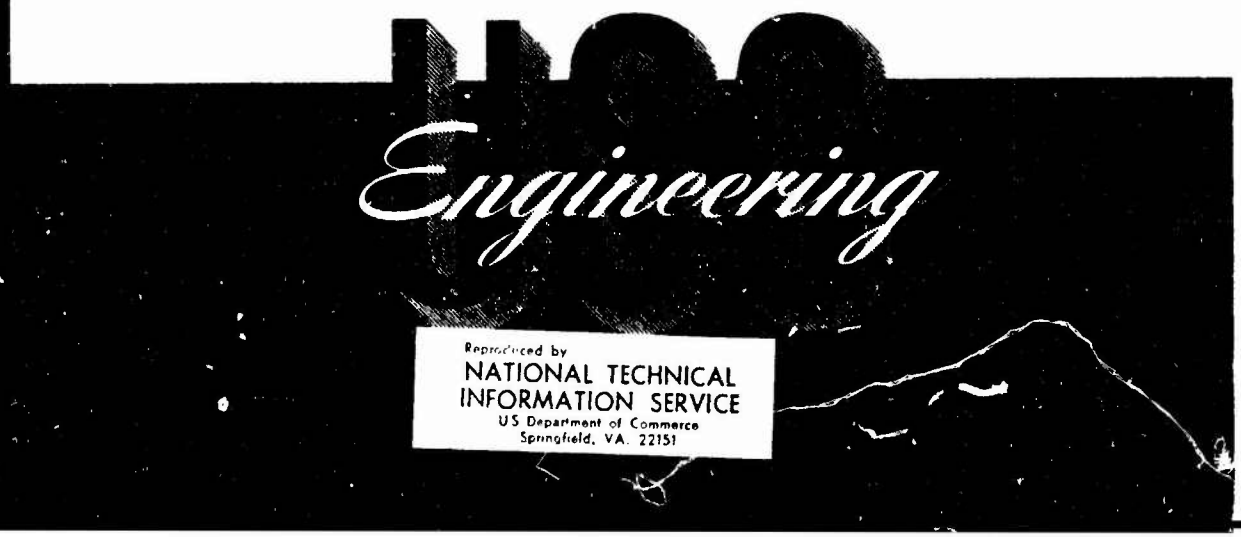

Security Classification

DOCUMENT CONTROL DATA - R & D

(Security classification of title, body of abstract and indexing annotation must be entered when the overall report is classified)

1 ORIGINATING ACTIVITY (Corporate author) Electronic Sciences Laboratory University of Southern California Los Angeles, California 90007	2a. REPORT SECURITY CLASSIFICATION UNCLASSIFIED 2b. GROUP

3 REPORT TITLE

IR WINDOW STUDIES

4 DESCRIPTIVE NOTES (Type of report and inclusive dates)

Scientific Interim.

5 AUTHOR(S) (First name, middle initial, last name)

Ferdinand Krüger and John H. Marburger

6 REPORT DATE	7a. TOTAL NO OF PAGES	7b. NO. OF REFS
15 March 1973	70	19

8a. CONTRACT OR GRANT NO	9a. ORIGINATOR'S REPORT NUMBER(S)
F19628-72-C-0275 b. PROJECT NO Task, Work Units Nos.	Quarterly Technical Report No. 3
c. DoD Element 6110D	9b OTHER REPORT NO(S) (Any other numbers that may be assigned this report)
d. DoD Subelement n/a	AFCRL-TR-73-0054

10 DISTRIBUTION STATEMENT

A-Approved for public release; distribution unlimited

11 SUPPLEMENTARY NOTES	12 SPONSORING MILITARY ACTIVITY
TECH, OTHER	Air Force Cambridge Research Laboratories (LQ) L. G. Hanscom Field Bedford, Massachusetts 01730

13 ABSTRACT

During this quarter, additional wavelength dependent calorimetric measurements of IR absorption in very pure GaAs have been made which indicate that a lower level of absorption coefficient is being reached for GaAs grown from the high temperature melt by conventional techniques. Experiments on strain annealing and purification of GaAs have been carried out in an effort to modify its absorption characteristics. The stress-strain properties of GaAs are under continuing investigation. Our ultra pure Alkali Halide production facility is now in operation and producing KCl powder as well as single crystals. A new technique for measuring surface absorption has been devised, and preliminary feasibility experiments completed. An important class of sum rules for the frequency moments of the multiphonon contribution to absorption coefficients has been discovered. Progress in other areas of IR window material preparation, characterization and growth is reported.

DD FORM 1 NOV 68 1473

UNCLASSIFIED
Security Classification

14 KEY WORDS	LINK A		LINK B		LINK C	
	ROLE	WT	ROLE	WT	ROLE	WT
IR Windows						
Alkali Halides						
III-V Semiconductors						
II-VI Semiconductors						
Thermal lensing						

IR WINDOW STUDIES

by

Ferdinand A. Kröger

and

John H. Marburger

Electronics Sciences Laboratory
School of Engineering
University of Southern California
Los Angeles, California 90007

Contract No. F19628-72-C-0275
Project No. 5621
Task No. 562108
Work Unit No. 56210803

Quarterly Technical Report No. 3

15 March 1973

Contract Monitor: Alfred Kahan
Solid State Sciences Laboratory

Sponsored by
Defense Advanced Research Projects Agency
ARPA Order No. 2055
Monitored by
AIR FORCE CAMBRIDGE RESEARCH LABORATORIES
AIR FORCE SYSTEMS COMMAND
UNITED STATES AIR FORCE
BEDFORD, MASSACHUSETTS 01730

ABSTRACT

During this quarter, additional wavelength dependent calorimetric measurements of IR absorption in very pure GaAs have been made which indicate that a lower level of absorption coefficient is being reached for GaAs grown from the high temperature melt by conventional techniques. Experiments on strain annealing and purification of GaAs have been carried out in an effort to modify its absorption characteristics. The stress-strain properties of GaAs are under continuing investigation. Our ultra pure Alkali Halide production facility is now in operation and producing KCl powder as well as single crystals. A new technique for measuring surface absorption has been devised, and preliminary feasibility experiments completed. An important class of sum rules for the frequency moments of the multiphonon contribution to absorption coefficients has been discovered. Progress in other areas of IR window material preparation, characterization and growth is reported.

CONTENTS

1. INTRODUCTION

The format of this report follows closely that of the first quarterly report in which projects are identified by codes keyed to the contract work statement.

The various categories are briefly

a) Crystal growth
b) Polycrystalline window fabrication
c) Mechanical properties of window materials
d) Window material defect characterization
e) Theory of residual IR optical absorption
f) Absorption measurement techniques
g) Theoretical evaluation of optical performance of windows

a.1 Effect of Oxygen and Other Impurites on IR Absorption in II-VI and III-V Compounds

James M. Whelan, Murray Gershenzon

During the last reporting period an attempt was made to acquire a variety of semi-insulating GaAs samples from laboratories which had had active programs on the preparation of high purity GaAs in the past 10 - 15 years, but had since discontinued these programs and switched to epitaxial growth. Willingness to cooperate is evident but the search for old samples is still underway.

Work on the use of zirconia oxygen pumps has progressed to the point where the detection limits for oxygen in gallium can be given for a temperature of 500°C. They are $1 - 3 \times 10^{-9}$ gm atom oxygen/gm atom of Ga for oxygen atom fractions of $2 - 4 \times 10^{-7}$. The uncertainty in the detection limit is due to the extrapolations made to zero time after pumping in and pumping out identical amounts of oxygen. It is anticipated that this difference can be reduced by improved corrections. Even with this uncertainty we note that the detection limit is approximately equivalent to one monolayer of oxygen on a cm^2 of GaAs.

The use of the zirconia pumps to remove oxygen from Ga solutions saturated with As prior to and during the growth of epitaxial GaAs has been achieved at 600°C. The film grown on a 211 substrate was smooth and of high quality. These features compare well with films grown by conventional means at temperatures 100 - 150°C higher. This is considered to be significant in the long run because advances in higher purities in the past have resulted from lowering the growth temperatures.

Construction of the horizonal solution growth reactor will be completed during the next reporting period.

a.2. Optimization of Alkali Halide Window Materials

P. J. Shlichta, R. E. Chaney

Status of Program: The ultimate goal of this part of the program is the determination of the effect of impurities and lattice defects on the optical and mechanical properties of KCl and other alkali halides. This will be done by testing as-grown crystals, both of the highest possible purity and with known concentrations of impurities. As of the present quarter, the purification system is operational and high-purity polycrystalline ingots of KCl are being prepared both for crystal growth at USC and for evaluation by other ARPA investigators. Final modifications are being made on the crystal-pulling apparatus and preparations are underway for the growth of crystals with {100} faces for optical absorption measurements. Plans are being made for extension of the present program to include the purification and growth of KBr crystals and the preparation of an atlas of infrared absorption spectra of alkali halide crystals.

Purification of KCl: As has been described in previous quarterly reports (1,2), KCl is being purified by a combination of (a) passage of solution through ion-exchange resins, (b) fractional crystallization, and (c) treatment of the molten salt with Cl_2 and HCl. The apparatus is designed so that, from the onset of purification until the crystal is grown, the material is kept from contact with potentially reactive metals or glasses and protected from contamination by airborne dust. Indeed, there is only one step in the process during which the material need be exposed to air at all.

(a) The ion-exchange system is operating as previously described (1,2) and is presently capable of producing several gallons of purified solution per day. This is more than we can at present use; therefore limited quantities of solution are available for use by other ARPA investigators.

(b) Purified solution from (a) is collected in one-gallon polyethylene bottles having two polyethylene stopcocks in the cap. The bottle is then disconnected from the ion-exchange system and transferred to a vacuum evaporator (a vacuum dessicator with a bell jar replacing the lid), wherein the solution-bottle stopcocks are opened and the solution heated under aspirator vacuum until enough water has evaporated to initiate crystallization. For reasons already stated (2), this first fraction of crystals is discarded by filtration through a milipore filter into one-gallon polyethylene wide-mouth jar which also has two polyethylene stopcocks in its lid. The jar is then returned to the vacuum evaporator and the solution evaporated until about two-thirds of the KCl has crystallized out. The jar is then removed and the remaining solution drained off and discarded. (In order to avoid the build-up of sodium as an impurity, the remaining solution is not, as described previously, recycled into the ion-exchange system.) It will be noted that, up to this point in the purification process, the solution is in contact only with polyethylene apparatus and inert gas and need not be exposed to air or dust.

(c) The jars are then opened and the KCl then transferred, in a clean bench, into vitreous carbon crucibles which are then inserted into the crystal growth chamber, which has been described in a previous report (2). The chamber is then attached to the gas-treatment system, shown in Figure 1. This system has been designed for maximum versatility in varying the gas treatment process. Cold traps C, D, and E can be used to trap out impurities in the gases used or the gases can even be distilled into the crystallization chamber. Cold traps F and G permit toxic or corrosive gases to be frozen out prior to absorption in the scrubbers. The molten KCl can be treated with a static atmosphere of HCl and/or Cl_2 via stopcock 17, or the gas can be flowed past or even bubbled through the molten KCl, via stopcock 18, and evacuated via stopcock 17.

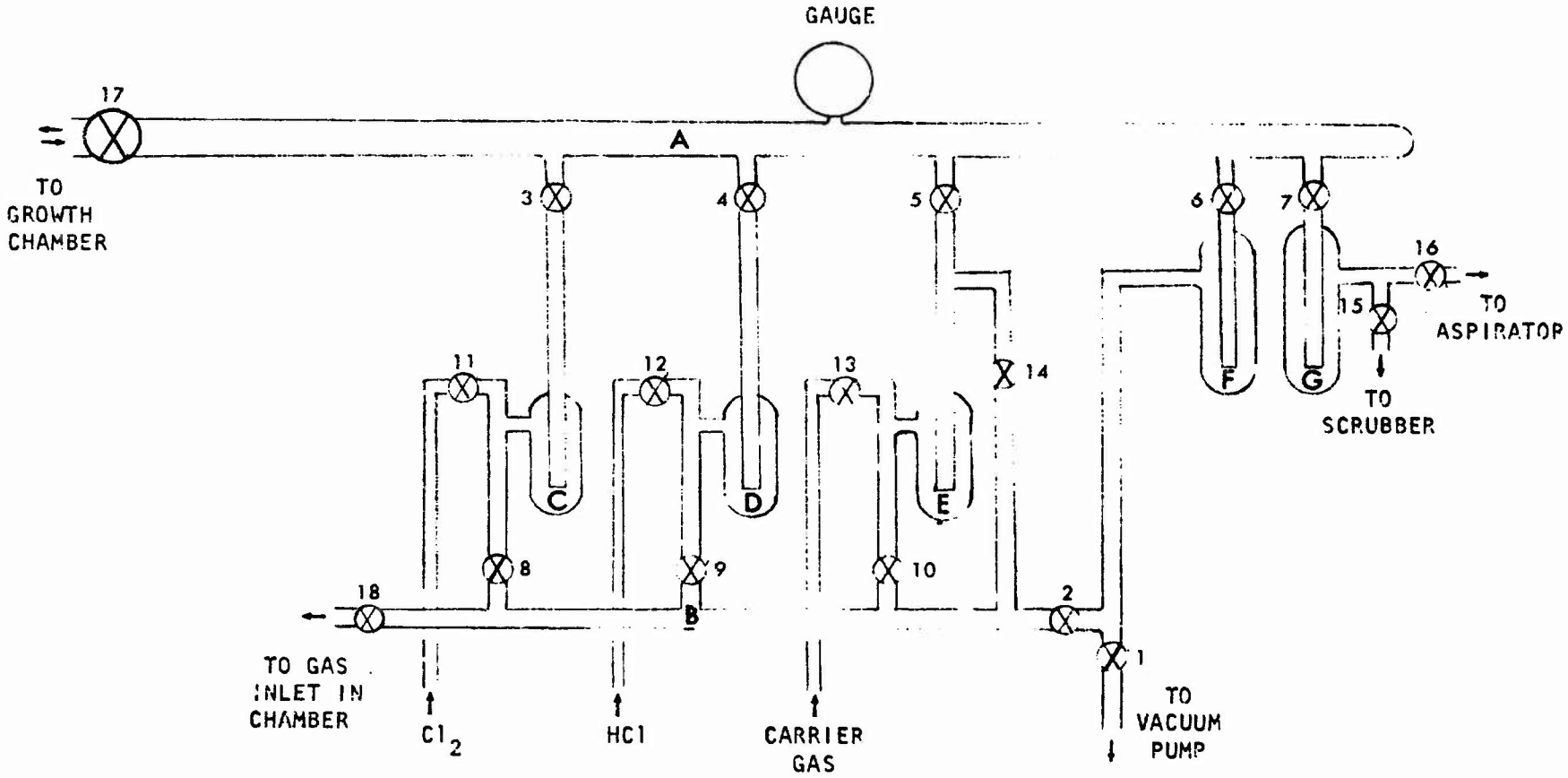

Figure 1: Gas treatment system for purification of KCl with HCl and Cl_2.

At present, to satisfy the needs of other ARPA investigators, we are preparing a series of polycrystalline ingots for use in forging studies. However, under normal procedure, the crystallization chamber would then be sealed, removed from the gas-treatment apparatus, and transferred to the crystal puller.

Growth of KCl Crystals: The Lepel crystal puller has been adapted to accomodate the chamber used for molten salt purification. Two additional modifications are now in progress. The present furnace, consisting of commercial hemicylindrical resistance elements, affords insufficient visibility for seeding. Therefore a fully transparent furnace, consisting of a coil of shielded nichrome wire with a radiation reflector (a quartz tube with a transparent gold film on its inner surface) (3), will be constructed early in the next quarter. The other modification, consisting of an auxiliary chamber mounted immediately above the growth chamber and connected to it by a vacuum ball valve, will permit insertion of seed crystals and removal of finished crystals without disturbing or contaminating the molten salt in the growth chamber. This modification will be described in detail in the next report.

Our first attempts at crystal pulling will be directed toward the production of <100> prisms with as-grown optical quality {100} faces. These will be used for calorimetric measurements of absorption coefficient.

Absorption Measurements (see f.1): Arrangements have been made for exchange of alkali halide crystals with other investigators. A high-purity NaCl crystal has been received from Prof. W.J. Frederick of Oregon State University, and is presently being used for calorimetric measurements. Arrangements have also been made for obtaining a purified KBr crystal from Prof. P.W.M. Jacobs of the University of Western Ontario.

Extension of Activities: It has been pointed out by Dr. Marshall Sparks, of Xonics Inc. (4), that KBr may be superior to KCl as

a 10.6 micron window material, provided its optical absorption is really as low as has been predicted for high-purity material. Because of the problem of chloride contamination and the fact that Br_2 is a far weaker oxidizer than Cl_2, it is presumed that KBr will be considerably harder to purify than KCl. It has, however, been demonstrated that treatment with HBr and Br_2 can successfully remove OH and other anionic impurities from KBr (5). Therefore, we are taking preliminary steps to include the growth of high-purity KBr crystals in our program. Thus far, we have constructed additional ion exchange columns and have made plans for modifying our ion-exchange and gas-treatment apparatus to include KBr purification.

At the suggestion of Dr. A. Kahan of AFCRL, we are making preliminary plans for the compilation of an atlas of impurity-caused infrared absorption spectra of alkali halide crystals. However, an examination of some of the references in the literature has convinced us that the species causing most of the observed absorption spectra have not been conclusively identified. We are therefore confining our compilation to positively identified spectra. It is not likely that any preliminary compilation will be available before October.

REFERENCES

1. Marburger, John H., et al. Electronic Sciences Laboratory, University of Southern California, "IR Window Studies", Quarterly Technical Report No. 1 (June-August 1972), Contract No. F19628-72-C-0275, ARPA Order No. 2055 (29 September 1972).

2. ibid, Quarterly Technical Report No. 2 (September-November 1972), to be published.

3. Thomas B. Reed (Lincoln Laboratories, M.I.T.), private communication.

4. Sparks, Marshall (Xonics Inc.), private communication.

5. Jacobs, P. W. M., and Menon, A. K., J. Chem. Phys. 49 (1968) 2920.

a.3 Growth of Crystals for IR Window Research

E. A. Miller and W. R. Wilcox

(Chemical Vapor Deposition of Bulk Gallium Arsenide Crystals)

During this reporting period, effort was devoted entirely to the open tube process. The system was in operation by December 15, 1972, as anticipated in the previous progress report.

In the initial experiment, resistance heating was employed for the gallium source and radio-frequency induction heating for the gallium arsenide substrate. Hydrogen gas was saturated with $AsCl_3$ in a temperature-controlled bubbler. Before insertion of the substrate, the H_2 + $AsCl_3$ was passed over the gallium source at 850°C so as to generate a crust of gallium arsenide. The substrate was then inserted and heated to about 900°C in order to etch it and remove any possible surface damage and oxide. The substrate temperature was lowered to 750°C and deposition continued for 16 to 24 hours. Figure 1 shows the rough surface produced on a {111} surface. This roughness was attributed to oxygen and/or water vapor permeation through several tygon tubing connections in the gas flow system. Some difficulty was also encountered in measuring and controlling the substrate temperature by radio frequency heating. As a consequence later experiments were performed with teflon tubing replacing the tygon and with resistance heating of the substrate.

Figure 2 shows the result of growth on a twinned {111} substrate at 775°C. A smoother deposit was obtained, although pits formed on the upstream end of the surface, possibly due to a small leak in the flowmeter. Note that the two twinned portions exhibited

different textures and growth rates. Figure 3 shows the result with a 805°C substrate temperature. The best deposit thus far was obtained, although elimination of the leak may have been responsible.

Presently all teflon joints are being replaced with glass to reduce further the probable oxygen/moisture content. Temperature controllers are also being installed on the furnace to permit control within $\pm$ 1°C. We expect the improved system to be operational by 15 March 1973. The optimum temperatures for deposition will be determined. Films of 1 to 2 mm thickness will be prepared and submitted for infrared absorption measurements. Dopants will be added to determine their influence on optical absorption.

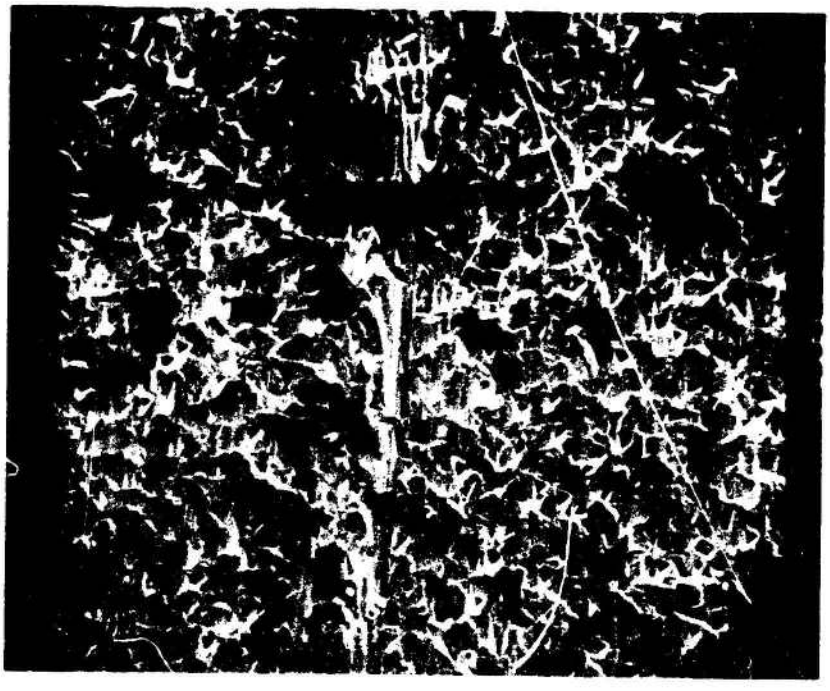

Figure 1. Scanning Electron Micrograph of Film Deposited on {111} Twinned Substrate, CVD 1 at 190X, 10 kV, 30° Tilt.

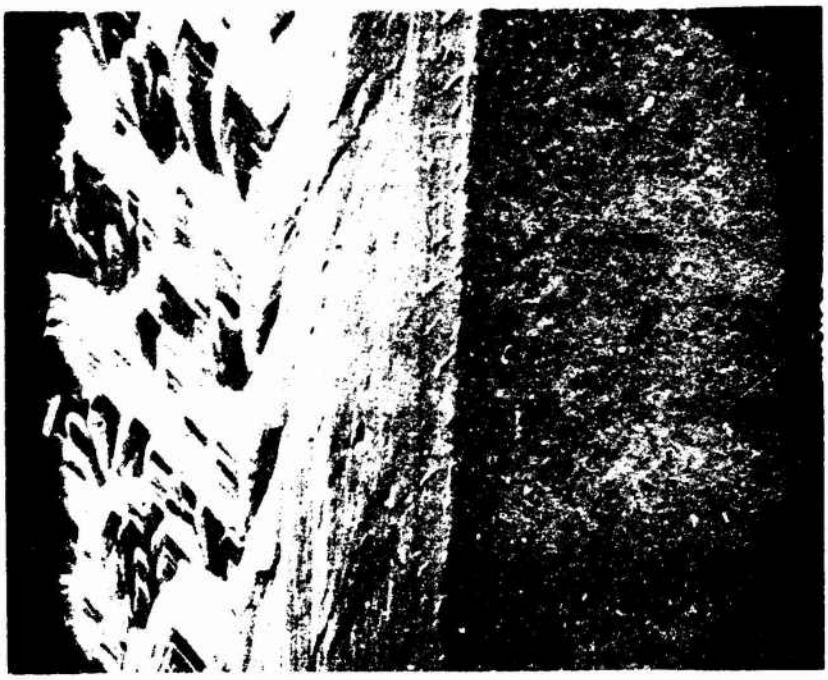

Figure 2. Scanning Electron Micrograph of Deposit on {111} Twinned GaAs Substrate. Run CVD 3, 200 X, 10 kV, 30° Tilt.

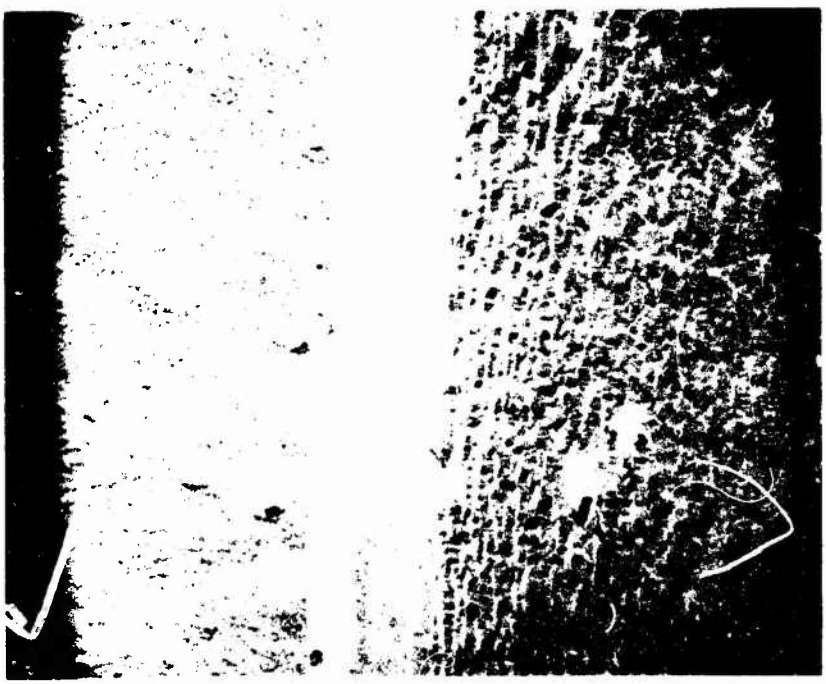

Figure 3. Scanning Electron Micrograph of Deposit on {111} Twinned GaAs Substrate. Run CVD 4, 180 X, 10 kV, 30° Tilt.

b.1 Fabrication of Polycrystalline IR Window Materials

Stephen M. Copley, James M. Whelan, V. Rana

This part of the program is concerned with producing polycrystalline samples of gallium arsenide and II-VI compounds by hot pressing the powder in the presence of a sintering aid.

The description of the hot press and its operating procedure has been given in a previous quarterly report. The hot press has been fabricated and is ready to go into operation.

GaAs powder for use in the hot press will be obtained by milling GaAs chips in a steel ball mill. Any iron or other metallic impurity picked up by the powder during this operation will be removed by acid leaching. The GaAs powder will be hot pressed in the presence of liquid arsenic and arsenic vapors.

The presence of liquid arsenic will facilitate the flow and rearrangement of particles in the initial stages of densification. Any oxide or sulfide present on the GaAs particles will be dissolved in the liquid As and reduced by contact with the graphite dies. During compaction, most of the As liquid will be squeezed out to the surface leaving behind a purer GaAs. Excess As will be removed by vaporization during subsequent annealing of the compact.

To check operation of the equipment, preliminary experiments will be performed using liquid gallium as a sintering aid. At higher temperatures, liquid Ga will be distributed along the grain boundaries in a manner similar to liquid As. Although it can not be removed by vaporization during subsequent annealing, it will only be present in a small amount and most of the liquid will be squeezed out of the compact during the pressing operation.

The same technique will be subsequently used to obtain polycrystalline compacts of II-VI compounds.

c.1 Mechanical Behavior of III-V and II-VI Compounds

Stephen M. Copley and V. Swaminathan

Mechanical Properties:

This investigation is concerned with the mechanical behavior of laser window materials. In our initial experiments we are studying the mechanical behavior of GaAs single crystals. We have obtained a melt grown single crystal doped with Si with a carrier concentration of 10^{18} cm^{-3}, and have prepared ⟨100⟩ oriented compression specimens with a goniometer and a precision cut-off wheel. Stress-strain curves will be obtained at 50 C° intervals starting at 550°C (above this temperature As loss becomes a problem) and continuing down to a temperature where no plasticity is observed. Stress-strain curves at 550, 500 and 450°C are shown in Fig. 1. By observing the slip offsets at the surfaces of the deformed samples, {111} ⟨110⟩ slip system which has previously been observed was found to be operative; however, there are indications that {110} ⟨110⟩ slip system may also be operating. These indications will be further verified. In the forthcoming weeks, the yielding behavior of ⟨111⟩ oriented samples will be studied. Then a comparison of the plastic behavior for the two orientations will be made.

Recrystallization

It may be possible to start with the absorption characteristics of a relatively high purity material in coarse grained polycrystalline form and to improve them by sweeping out the volume with grain boundaries. Such sweeping can be obtained by deforming the material and then annealing it to produce recrystallization. By transferring the solute atoms from the volume to grain boundaries the symmetry of their environment is changed and thus

changes in absorption characteristics may occur. With this idea in mind, recrystallization experiments on the Si doped material are being carried out. Annealing of samples with 3% to 4% deformation, in sealed quartz tubes at 600°C for 3 hours, has not produced the desired result. It is hoped that it will be possible to recrystallize severely deformed samples by annealing them at very high temperatures. Annealing of a sample with 15% deformation at 800°C is in progress.

Optical Absorption

In order to see the effect of recrystallization on optical properties, attempts have been made to measure the optical absorption of the deformed and annealed samples. Due to free carrier absorption, no meaningful results could be obtained. Therefore a Cr-doped GaAs sample has been obtained from Bell-Howell. A Hall experiment has been done on the sample and a resistivity of $10^9 \Omega$ cm and a carrier concentration of $10^8/cm^3$ have been measured. The optical absorption of this sample lies in the range of 0.01 to 0.05 cm^{-1}. After establishing recrystallization conditions, experiments will be carried out on this sample.

Transmission Electron Microscopy

In the last report problems regarding dirt accumulation and precipitation during foil preparation were mentioned. These precipitates obscured contrast. This problem is solved and clean thin foils can now be prepared.

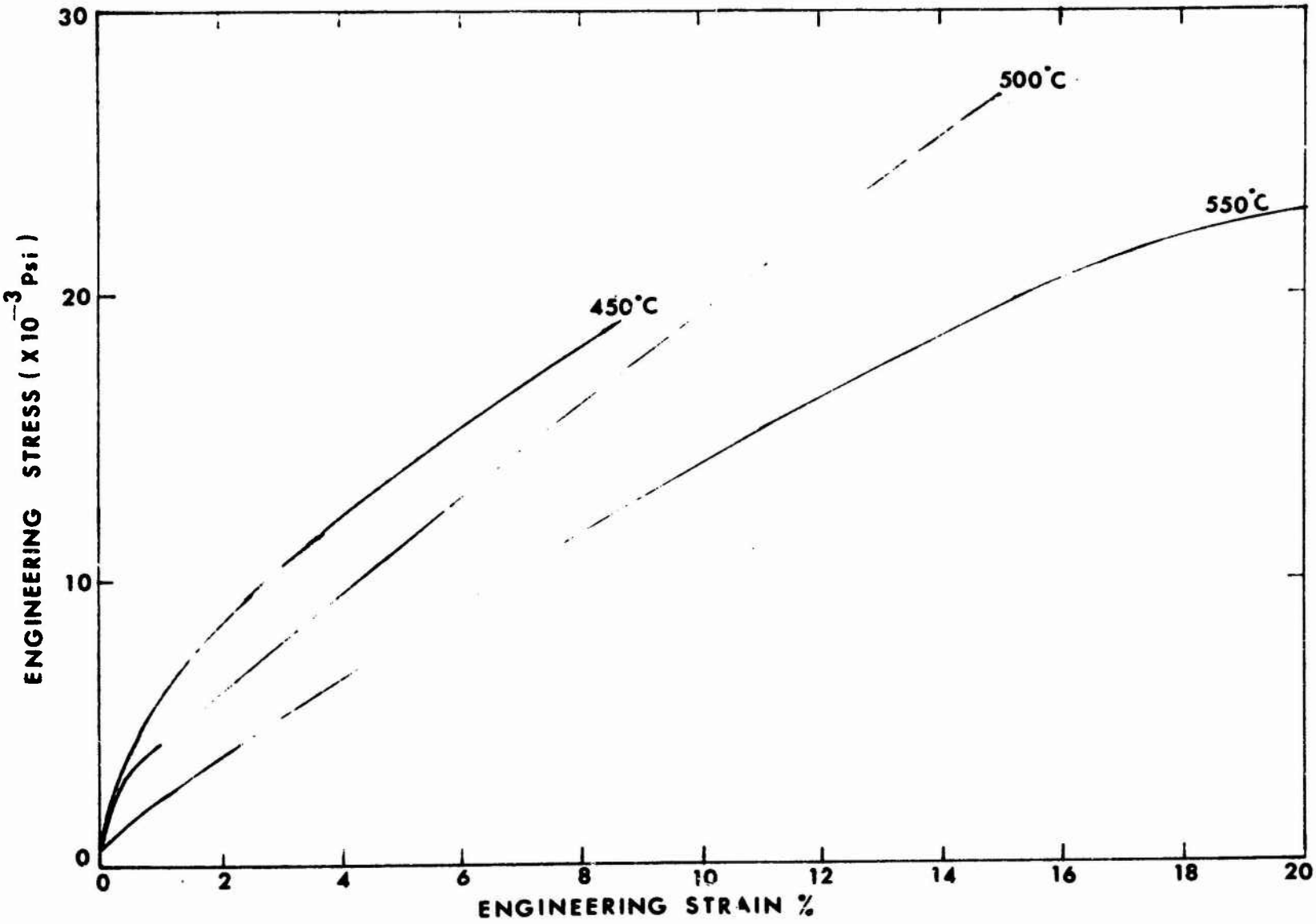

Fig. 1 Engineering Stress-Engineering Strain Curves for (100) oriented Si doped GaAs at Various Temperatures. 1/w = 1.5, Stress Rate = 20 psi/sec.

d.1 Surface and Interface IR Absorption

Clarence Crowell, T. Mangir, S. Joshi

We are attempting to correlate surface and interface contributions to IR absorption with electrical measurements of the conductivity and capacitance of illuminated GaAs MIS structures. To this end we have been attempting to construct the device configuration shown in Fig. 1. This is an MIS structure which uses air as dielectric. From this structure we hope to get information on the air-GaAs interface. We have attempted to establish the thickness of the air gap by metal film spacers deposited on the GaAs surfaces under investigation. During device operation this film is intended to be contacted by a metallized registered pattern deposited on an optically flat insulating substrate. The substrate is also used to support the gate electrode. The most critical requirements are that the gate electrode and GaAs surfaces be as flat as possible and that they be mounted stably and as close as possible to each other. This maximizes the capacitive effects of the GaAs surface states and of the depletion layer under the GaAs surface.

To date we have attempted to produce flat surfaces of GaAs but have not achieved consistent success. Our current preparation techniques are as follows:

1. Boules of GaAs are mounted with apiezon W wax and cut into wafers with a diamond impregnated .022" metal saw. This procedure is supposed to produce a damaged layer of the order of .004" thick (Frank, 1967).
2. After degreasing 10 min. in warm TCE and 10 min. in boiling methanol, the surfaces are etched in a $1\,H_2O_2 : 3\,H_2SO_4 : 1\,H_2O$ solution for 6-7 minutes (Cunnell, 1960). This step removes ~.006" and should remove most of the damage associated with sawing.
3. The wafers are then mounted on a polishing block and given a chemical-mechanical polishing with mirrolite (Materials Research Corporation) approximately one hour. This step removes ~.001". The major action of this compound is chemical polishing. The sample pressure is ~ 20 lbs/sq. in..

4. On completion of the polishing, the samples are washed with neutralizer soap and DI water. Subsequently the wafers are removed from the polishing block with hot TCE and methanol and rinsed thoroughly in DI water.

The surfaces then are flat to the eye and under a multiple beam interferometer appear to have an average roughness ~ 1000 Å in 0.15". At this point we have attempted to etch the surfaces to remove the ~1μ surface damage presumed to be there and to prepare the back surface for an Au-Ge (13% eutectic) ohmic contact alloyed at 450°C. The sample should be etched a second time in preparation for deposition of the metal spacers which are also intended as Schottky barriers for diagnosis of the bulk semiconductor doping. It appears that our currently prepared samples either are overetched or that the material has been damaged in some manner. During etching our GaAs surfaces rapidly develop a wavy texture and show signs of preferential etching. This was not true of a wafer used earlier to make Schottky diodes, nor have we currently succeeded in producing Schottky barriers with current-voltage characteristics that matched those produced earlier. Further controlled etching experiments are in progress and a variety of starting materials will be used.

The lack of surface flatness has precluded taking any significant MIS measurements. We plan to reduce the size of the wafer and conduct s systematic study of mounting systems which will produce and maintain the close spacing configurations required. We also plan to study MIS systems in which the insulator is SiO_2. This will permit the basic phenomenon to be given at least a qualitative investigation for a potentially useful interface even if it is not the GaAs-air interface. Corresponding measurements on surfaces that still have damage due to surface polishing and on metal-GaAs interfaces should also be of interest.

As part of our role of providing electrical characterization of materials we have made Hall measurements on some of the high resistivity materials used for the bulk optical absorption studies. The lowest loss material showed virtually intrinsic carrier concentration, a Hall mobility of 2140 cm^2/vot-sec, and a carrier activation energy of 0.69 eV. We have not yet made measurements on the Bell & Howell materials because the Van der Pauw sample we cut has

a grain boundary which is apparent under the infrared microscope but is not visible on the polished material.

References

Daniel R. Frankl: " Electrical Properties of Semiconductor Surfaces "
Pergamon Press, 1967.

F. A. Cullen, J. T. Edmon, W. R. Harding (1960)
Solid State Electronics 1, 97.

Materials Development Corporation
Los Angeles, California 90045

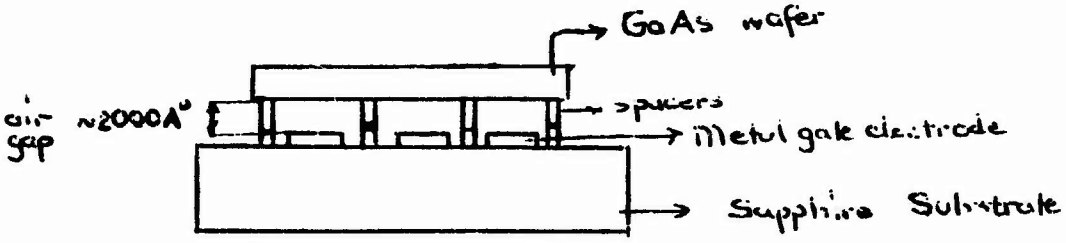

Figure 1a: Side View

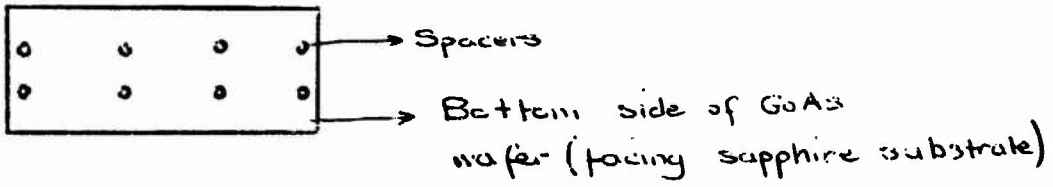

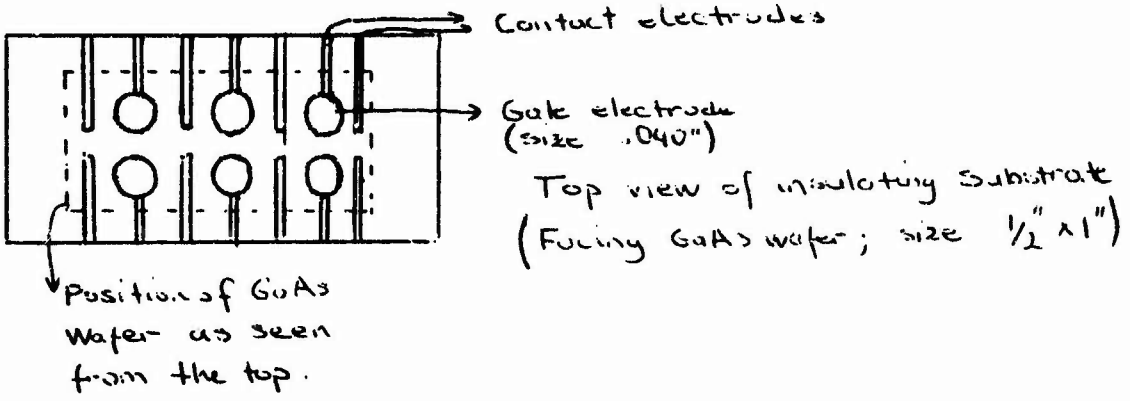

Fig 1. Device Configuration for GaAs-air interface study

d.2 STUDY OF DEFECTS IN II-VI COMPOUNDS

F.A. Kroger, M. Gershenzon, S.S. Chern, and H.R. Vydyanath

1. Cd^* Tracer Self Diffusion

Cd^* self diffusion studies in CdTe-In as fp_{Cd} were extended to more strongly doped material, viz. to CdTe. $10^{18} cm^{-3}$ In. The effects observed at low indium concentrations now reappear more strongly. At high p_{Cd} diffusion by $Cd_i^{\cdot\cdot}$ is further suppressed, that by $V_{Cd}^{'}$ is increased. At low p_{Cd}, the main charge compensating species is singly charged (Te_i or $V_{Cd}^{'}$) at low ([In], but doubly charged ($V_{Cd}^{'}$) at high [In]. The Cd^* tracer self diffusion under these conditions probably involves $V_{Cd}^{''}$.

The shape of the D_{Cd}^* isotnerm for CdTe. 10^{18} In indicates an increase in the donor activity of In from medium to high p_{Cd} beyond the variation expected for a change in charge compensation from $V_{Cd}^{'}$ or $V_{Cd}^{''}$ to $e^{'}$. A related effect was observed in our Hall effect measurements, the donor activity increasing with increasing temperature by a factor of 2-3. Both effects can be explained if indium changes sites, from Cd sites at low p_{Cd}, low T, to interstitial sites where it will be a multiple (double or triple) donor. For a donor multiplicity m, the site transfer reaction is

$$In_{Cd} + V_i^{x} \rightarrow In^{m\cdot} + V_{Cd}^{''} + (m-e)\ e^{'}$$

with m = 2-3 (dot = effective charge +, dash = effective charge -, cross = effective (charge 0). We shall try to determine the value of m as well as the equilibrium constant of the above reaction.

2. Chemical Diffusion Establishing Non-stoichiometry

The information on self-diffusion obtained in our tracer experiments can be used to explain chemical diffusion involved in varying the stoichiometry of the crystals. In CdTe and CdTe - In, Cd is the fastest diffusant under all conditions.

Two complications occur:

(a) Since the diffusing Cd-species (Cd_i or V_{Cd}) are charged, their movement has to be in combination with electrons: we are dealing with ambipolar diffusion.

(b) At high p_{Cd}, $Cd_i^{\cdot\cdot}$ may or may not be the major species, $V_{Te}^{''}$ being also present, with $[V_{Te}^{''}]$ < or > $[Cd_i^{\cdot\cdot}]$. At low p_{Cd} we have Te_i^{x}, $Te_i^{'}$ in addition to the Cd^{*} carrying species, $V_{Cd}^{''}$.

If the concentrations of the Te-defect species are larger than those of the Cd - carrying species, we have the complication that after or while Cd has diffused or is diffusing, the Te - species have to be formed by secondary reactions. At high p_{Cd}:

$$Cd_i^{\cdot\cdot} + V_{Cd}^{''} \rightarrow Cd_{Cd}^{x}$$

$$0 \rightarrow V_{Cd}^{''} + V_{Te}^{\cdot\cdot}$$

$$\overline{\qquad\qquad\qquad\qquad} +$$

$$Cd_i^{\cdot\cdot} \rightarrow Cd_{Cd}^{x} + V_{Te}^{\cdot\cdot}$$

At low p_{Cd}

$$V_{Cd}^{''} \rightarrow V_{Cd}^{x} + 2e^{'}$$

$$V_{Cd}^{x} + V_{Te}^{x} \rightarrow 0$$

$$Te_{Te}^{x} + V_i^{x} \rightarrow Te_i^{x} + V_{Te}^{x}$$

$$\overline{\qquad\qquad\qquad\qquad} +$$

$$V_{Cd}^{''} + Te_{Te}^{x} + V_i^{x} \rightarrow Te_i^{x} + 2e^{'}$$

Various authors reported asymmetrical behavior, relaxation times τ_+ measured with increasing p_{Cd} being from 1.5 to 12 times smaller than those (τ_-) measured with decreasing p_{Cd}. This asymmetry is probably due to the secondary reactions.

Two types of effects may occur:

(a) rates of the secondary reactions of diffusion processes involving them, are of the same order as those for the Cd diffusion.

(b) nucleation problems for the annihilation of vacancies by the Schottky reaction, giving rise to vacancy clusters $(V_{Cd}\ V_{Te})_n^x$ or dislocation loops. The smaller asymmetries (by a factor 2-3) may be due to (a).

It seems likely that only nucleation problems explain the large asymmetry effect. This finds support in a two-stage relaxation observed by Russian authors. Such clusters deserve further attention since they may give rise to light scattering.

In our experiments we sometimes find moderate asymmetry, with $\tau_+ < \tau_-$, but symmetrical behavior has also been found. We are trying to find which factor in the previous history determines the behavior, and how T depends on p_{Cd}.

3. Tellurium Self Diffusion

It is well established, that Te^* tracer selfdiffusion at low p_{Cd} involves neutral defects, Te_i^x, giving $D_{Te}^* \propto p_{Cd}^{1/3}$ corresponding to Te^* diffusion by $V_{Te}^{\cdot\cdot}$. At lower temperatures D_{Te}^* still increases with increasing p_{Cd}, but the slope is < 1/3. Apparently we are in the transition from $D_{Te}^* \propto p_{Cd}^{-1}$ to $\propto p_{Cd}^{1/3}$.

4. Density Measurements on CdTe.In

The accuracy of density measurements turns out to be insufficient to justify conclusions as to the main mechanism of compensation: by V_{Cd} or Te_i. A previous conclusion that Te_i is the dominant species therefore cannot be trusted.

5. CdS - Ag

Previous Hall effect studies on Ag-doped CdS proved unreliable due to the in-diffusion of unwanted impurities (Cu?) during preparation of the samples. This has been avoided by preparing doped samples by equilibration of CdS with $(Cd, Ag)_l$ alloys. The alloys act as a sink for the unwanted elements, thus preventing contamination. High temperature Hall effect studies on crystals with $2 + 10^{17}$ to 10^{19} Ag/cm^3 at high p_{Cd} show that under such conditions Ag is a donor.

Since Woodbury found the silver solubility to be $\propto a_{Ag}^2$, the donor species must contain two Ag atoms; it is probably $(Ag_i\ Ag_{Cd})^x$, ionizing according to $(Ag_i\ Ag_{Cd})^x \rightarrow (Ag_i\ Ag_{Cd})^{\cdot} + e'$.

At all but the lowest Ag concentration the electron concentration $\propto [Ag]^m$ with $m = 1/2 - 1/3$. The electrons are minority species, charge compensation of the main silver species, $(Ag_i\ Ag_{Cd})^{\cdot}$ involving an Ag acceptor (Ag'_{Cd}).

Our results contradict an earlier conclusion by Woodbury that at high p_{Cd} silver is electrically inactive, it being present as a neutral species. The Ag doped samples will also be measured at low p_{Cd} (in sulphur vapor), a condition for which initial experiments show that Ag acts primarily as an acceptor.

e.1. Theoretical Studies of Absorption Mechanisms in IR Window Materials

Robert W. Hellwarth, M. Mangir

In the last quarterly report we summarized a theoretical first step for the eventual exact calculation of multi-phonon absorption[1] in crystals whose macroscopic electric moment M_x (in some direction x) is linearly related to its ionic x-coordinates x_i (i labels the ions) by

$$M_x = \Sigma_i e_i x_i \qquad (1)$$

where the effective charge e_i on the ion i includes its nuclear charge and the effects of the adiabatic following of its nuclear motions by all the electronic charges. The approximation (1) is widely thought to be valid for alkali-halide, and other strongly polar, crystals, but its applicability to cubic III-V and II-VI window materials is uncertain.

In this quarter we:

a) examined the magnitudes of important terms left out of the first-step calculations done previously. With the aid of sum rules which we have discovered, we were able to show that these difficult neglected terms were definitely comparable to those already calculated and,

b) sought possible experimental methods to verify whether the "linear moment" approximation (1) is valid for calculating the absorption wing of a given crystal, or whether n-phonon absorption with $n>>1$ arises from terms in M of order x_i^2 or higher, as well as from anharmonic lattice forces. A study of the often contradictory literature on the subject has not clarified the issue. However, the temperature dependence of various weighted averages over frequency of the absorption coefficient and refractive index may provide the wanted clues.

a) Sum rules for IR absorption using "linear moment" approximation.

In our work of the last quarter we separated the IR susceptibility χ into terms representing the response of an individual ion coordinate x_i to a force on the coordinate x_j

$$\chi(\omega) = V^{-1} \Sigma_{i,j} e_i e_j g_{ij}(\omega) \tag{2}$$

and then assumed that i and j must represent an ion pair in a unit cell, otherwise the response g_{ij} was zero. We now show that these inter-cell responses must contribute comparably.

There is a well known quantum mechanical formula for the ion response functions appearing in the susceptibility function:

$$g_{ij}(\omega) = \frac{\hbar^{-1} \Sigma_{m,n,} \langle m|x_i|n\rangle \langle n|x_j|m\rangle \omega_{nm} P_m}{\omega_{nm}^2 - (\omega + i\epsilon)^2} \tag{3}$$

$$= g_{ij}^*(-\omega) = g_{ij}(\omega).$$

Here m labels the states $|m\rangle$ in the volume V, having energies $\hbar\omega_m$ ($\omega_{nm} = \omega_n - \omega_m$), and probabilities of occupation P_m. If the ions in V interact through a potential v that is a function of the ion position coordinates only, we have been able to derive simple expressions for the following "moments" of the imaginary part g_{ij}'' of the complex g_{ij} functions:

$$\int_0^\infty \omega^n g_{ij}''(\omega)\, d\omega, \qquad n = -1, 1, 3, 5 \tag{4}$$

and

$$\int_0^\infty \omega^m \coth\left(\frac{\hbar\omega}{kT}\right) g_{ij}''(\omega)\, d\omega, \qquad m = 0, 2, 4. \tag{5}$$

When n=1 in (4) one obtains the analogue of the well-known Thomas-Kuhn-Reich sum-rule for atoms. For multi-phonon absorption we have made most use of the following typical exact relation:

$$\int_0^\infty \omega^3 g_{ij}(\omega)d\omega = \frac{\pi}{4m_i m_j} \left\langle \frac{\partial^2 v}{\partial x_i \partial x_j} \right\rangle + i \neq j \qquad (6)$$

where m_i is the mass of the ion i. If v is a sum of two-body potentials v_{ij} then it is clear that $\partial^2 v/\partial x_i^2$, which appears in the self-response terms, is of order $[\partial^2 v_{ij}/\partial x_i \partial x_j]$ times [the number of nearest neighbors], at least if the forces are short-range. That is, many cross-terms g_{ij}, $(i \neq j)$ are clearly important compared to g_{ii}, unless light ions sit in a cage of heavy ions, whence the $m_i m_j$ denominator singles out the light-ion self-response.

b) Nonlinear moment effects.

Preliminary studies of this quarter indicate that the temperature dependence of averages such as (4) and (5) could be determined experimentally, and compared with the formulae such as (6) based on (1), and with formulae modified by the addition of nonlinear terms to (1), to determine whether the "linear moment" approximation is valid.

During the next quarter we plan to exploit the sum-rules further to estimate wing absorption, and to collaborate with the experimental projects in an effort to determine the role of nonlinear moments in the GaAs wing absorption.

f.1 Techniques for Indirect Measurement of Small Absorptive Losses

William H. Steier, S. T. K. Nieh, R. Joiner

I. Wavelength Dependent Calorimetry

Calorimetric measurements of the absorption coefficient of several low loss GaAs samples have been made over the wavelength range from 9.2 to 10.9μ. A large CO_2 laser which can be line-tuned through this band is used as a source for the measurements. The measurement technique and experimental setup have been described in earlier reports.

The results for three samples are shown in Figure 1. The description of each sample is given in Table 1. Each point on the absorption vs wavelength curve is the average of three or more separate measurements. The reproducibility of this average and hence the expected accuracy of the measurements is better than $\pm$ 3%. There are no experimental points between 9.84μ and 10.11μ as the laser output is too low in this region.

There is a definite similarity between the three curves, although the doping and growth of the boules are quite different. The Bell and Howell material is Cr doped and grown by the Czochralski technique. The USC material is un-doped and grown by the horizontal Bridgeman technique. It is hoped that the observed structure will shed some light on the cause of the residual losses in GaAs. It is premature, however, to make definite interpretations of the results without further data.

As a first step in this direction, we are planning to determine if the data is temperature dependent. A number of probable absorption mechanisms are temperature dependent, e.g., intrinsic multi-phonon absorption and impurity induced phonon absorption. The temperature dependence of multiphonon absorption due to a nonlinear moment is expected to be higher than that due to an anharmonic lattice. The absorption due to particulates or precipitates is relatively temperature independent. By studying the temperature dependence of the absorption vs wavelength curves we hope to be able to gain further insight into the basic mechanisms involved.

Most of the above temperature dependent phenomena vary approximately as $e^{\frac{-h\nu}{kT}}$. With $h\nu$ corresponding to a 10μ wavelength, a change in temperature from $300^{\circ}K$ to $400^{\circ}K$ should mean a factor of 3.4 change. Hence, it is expected that a $100^{\circ}C$ increase in sample temperature should make a readily observable change in α if the basic mechanism is one of the temperature sensitive ones described above. This experiment is now being prepared.

II. Computer Studies:

We are currently doing a computer simulation of the 3-dimensional heat flow during an adiabatic calorimetric measurement of samples of cylindrical, rectangular and arbitrary shapes. The purpose of this work is to determine the limitations of the assumptions used in the calorimetric measurements. This theory assumes that after an initial transient, the entire sample heats with the same heating rate. This

appears to be rigourously true only in cylindrical samples heated by a symmetric laser beam in the sample center. The effect of non-cylindrical samples, off-center heating, and higher order modes in the laser beam are unknown. For our initial work we have obtained the heat flow program developed at AFCRL by Parke and are in the process of converting it to be run on our IBM 360. We are also obtaining a copy of a much more general program, HEATING-3, developed at Oak Ridge National Laboratory which will cover samples of arbitrary geometry.

TABLE 1 -- Sample Information

Sample No.	EPD Cm^{-2}	ρ Ω -cm	Method of Growth
EMC 6012B*	9.5×10^4	2.2×10^7	Czochralski, Cr doped
EMC 6050T*	2.7×10^4	3.2×10^7	Czochralski, Cr doped
WA 1000**	--	$\sim 10^8$	Horizontal Bridgeman, undoped

* These samples were kindly provided by A.G. Thompson of Electronic Materials Corporation, Pasadena, California.

** Grown by Worth Allred at U.S.C.

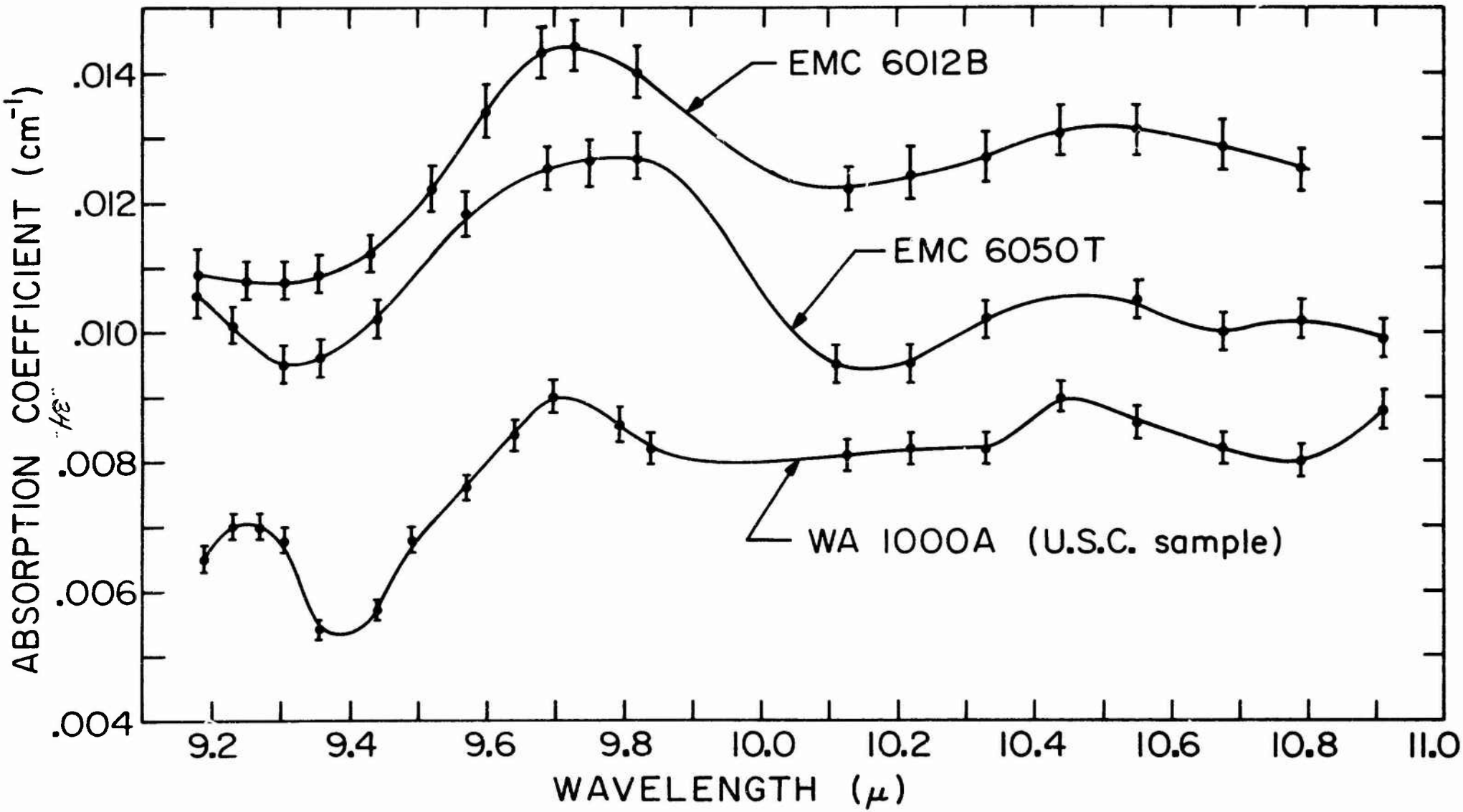

FIGURE 1. GaAs Absorption vs. Wavelength

3/23/73 J.S. Parks

f.2 Alkali Halide Surface Studies with Acoustic Probe Techniques

Joel Parks, Ted Colbert

New techniques are being developed to study induced temperature changes at material surfaces with a combined sensitivity and time response exceeding present thermal detectors. These techniques will be referred to as acoustic temperature detection, and they rely upon an accurate measurement of the induced phase variation of an acoustic surface wave which results when the wave propagates across a region having a different surface temperature. In these experiments, temperature changes will result from the absorption of 10.6μ radiation in alkali halide crystals.

The thermal detection scheme is shown in its simplest form in Figure 1. The material sample under study is a disk the order of 1 cm diameter and 3-5 mm thick which is capable of sustaining surface wave propagation and whose elastic coefficients and their temperature variations are known or measurable. Figure 1 depicts two acoustic wave interdigital transducers which serve as the transmitting and receiving components of an acoustic transmission line. This type transducer is composed of two sets of interspaced metallic fingers and is required to excite a well defined acoustic wave from which phase information can be sensitively detected and accurately analyzed. As discussed below, this transducer technique does not limit material studies to piezoelectric crystals. Measurements are performed by allowing the heating process to change the surface temperature of the material in the wave path and detecting the induced phase change.

The unique features of acoustic temperature detection arise from the following properties:

(a) The acoustic wave of width ~1mm propagates along a material surface extending a distance into the

material which is less than an acoustic wavelength. This depth can be varied by using different frequencies to differentiate between surface and bulk effects.

(b) The temperature variation of material elastic coefficients is large enough to produce a measurable phase change for temperature changes in the millidegree range. As shown below, this permits the measurement of absorption coefficients in the 10^{-3}-10^{-5} cm^{-1} range.

The following sections of this report review:

(1) calculations of induced phase changes resulting from the absorption of 10.6μ radiation in crystal quartz and sodium chloride,

(2) experiments to study the sensitivity and time response of acoustic temperature detection; and the generation of surface waves on nonpiezoelectric samples.

1.1 Calculations of Acoustic Temperature Detection in Crystal Quartz and NaCl

Calculations have been carried out to investigate the theoretical sensitivity of acoustic temperature detection in a well studied material, crystal quartz, and in an alkali halide material of interest, NaCl. In both cases the change of temperature at the crystal surface is generated by the absorption of 10.6μ radiation. The phase of an acoustic wave is defined by the integral

$$\Phi = \int k\,ds = \int \frac{\omega}{v_{so}}\, n(T)\, ds$$

along the propagation path, given the acoustic frequency ω, ambient speed of propagation v_{so} and an acoustic index n(T) depending on the surface temperature T. For small temperature changes, n(T) and the path increment ds can be expressed in terms of the velocity temperature coefficient $\alpha_2 = -\left[\frac{1}{v_s}\frac{dv_s}{dT}\right]$ and the thermal expansion coefficient α_1, respectively. The coefficient α_2 has been measured for crystal quartz[1], however an auxiliary computer calculation designed by Dr. K. Lakin was used to provide this parameter for NaCl. This program calculates α_2 as a function of angle in the XY plane and since this is the first time this information is available, it is presented in Figure 2. The phase change for a wave travelling through a heated region between two transducers separated by a length 2a is given by

$$\Delta\Phi = \left[\Phi - 2\pi\left(\frac{2a}{\lambda_s}\right)\right] = \frac{2\pi}{\lambda_s}\cdot 2\cdot \int_0^a (\alpha_1+\alpha_2)\,\Delta T(\rho)\, d\rho$$

in which the temperature change ΔT and the path variable are written in terms of the radial variable ρ assuming cylindrical symmetry.

The temperature change at the surface of a disk sample is calculated from a steady state heat equation driven by absorbed radiation propagating in the $\hat{z}$ direction normal to the disk surface. The thermal source term introduces the radiative absorption coefficient $\beta\ cm^{-1}$ and the heat equation is written

$$\nabla^2 T = -\frac{\beta}{\kappa}\frac{\langle P\rangle}{\pi S^2} T e^{-(\rho/S)^2} e^{-\beta z}$$

Here the thermal conductivity κ, transmission coefficient T, radiative power $\langle P\rangle$ and gaussian beam size S are source term parameters. This equation is solved subject to the boundary conditions that the normal temperature gradient vanishes at the faces of the disk sample. The sample is assumed to be edge cooled, and radiative and convective cooling of the disk faces are neglected.

The results for crystal quartz, which strongly absorbs at 1.06μ ($\beta > 200 cm^{-1}$), and for weakly absorbing NaCl ($\beta \sim 10^{-3} cm^{-1}$) are given in Figures 3 and 4. These graphs show the phase change $\Delta\Phi$ radians and temperature change $\Delta T\ ^{\circ}C$ as a function of 10.6μ power. The quartz calculations indicate the possibility of detecting millidegree temperature variations at radiative power levels $\sim 50\mu$watts. This possibility rests upon the detection of a phase change as small as $\sim 10^{-3}$rad which can be readily achieved using available electronic equipment, e.g. Hewlett Packard Vector Voltmeter 8405A.

The NaCl calculations support the feasibility of using acoustic temperature detection to measure small absorption coefficients with controllable 10.6μ power levels (0.1-1 watt). It is important to stress that the utility of this technique is based upon

(1) the sensitivity inherent in a null measurement,

(2) the ability to probe surface volumes at a depth of $\lesssim 1000A^{\circ}$ and bulk material at depths $\gtrsim 100\mu$,

(3) the reduction of data to a theory which involves the radiative absorption coefficient in a concise analytical form.

1.2 Initial Experiments to Develope Techniques for Acoustic Temperature Detection

The experimental effort is proceeding towards two initial goals

(a) to demonstrate the sensitivity of the acoustic measurement technique and investigate the range of linear response or additional limiting factors,

(b) to propagate acoustic surface waves on single crystal NaCl and study the propagation characteristics.

The progress in each of these projects is discussed below.

1.2a Acoustic Temperature Detection on Crystal Quartz Samples

The methods of acoustic wave phase measurements on heated surfaces are being studied with Y-cut crystal quartz samples. This material is extremely useful for initial studies of this technique because as a thoroughly investigated piezoelectric crystal its parameters have been measured in detail and the use of interdigital transducers is simplified. Quartz is heavily absorbing at 10.6μ and thus easily heated by modest CO_2 laser power levels. Experiments are beginning which will provide measurements at the lowest radiative power levels to indicate limitations to the sensitivity by material parameters and differential phase detection methods. A calibrated attenuator has been constructed for this purpose using a pair of Germanium Brewster angle windows. The CO_2 laser will be operating in a Q-switched mode which will also allow time response measurements.

Figure 5A,B shows a quartz sample with an interdigital transducer configuration composed of three transducers which was constructed in the laboratory of Dr. K. Lakin. In this case the 10.6μ beam is positioned to irradiate the surface within only one pair of transducers.

The center transducer transmits acoustic waves in both directions and by measuring the phase difference between waves received at the outer transducers a measurement of the radiatively induced phase change is obtained. In this configuration changes in the sample ambient temperature and oscillator frequency drift and instability are nulled out.

1.2b Acoustic Wave Propagation on NaCl Surfaces

The interdigital type transducer is necessary to achieve accurate, sensitive measurements of the acoustic wave phase, however this transducer excites and detects waves only when bonded to piezoelectric surfaces. Since the alkali-halide materials have cubic symmetry, it is necessary to develope an alternative interdigital transducer arrangement.

There are several techniques available which are capable of coupling waves to a nonpiezoelectric surface after these waves are initially excited on a piezoelectric material. These include:

(a) mounting a transducer on a piezoelectric material and then coupling acoustic waves through a fluid interface to the detector surface

(b) sputtered thin films, such as ZnO, which become oriented when deposited on the detector material surface and which then serve as the base for the transducer

(c) solution growth or chemical vapor deposition of a piezoelectric surface on areas of the sample substrate which will then serve as the transducer base.

Since the fluid coupling technique does not require that the surface be exposed to any contaminants generated by the processes necessary to deposit the transducers, it has been chosen for the initial

experiments. This technique has been used[2] successfully on other nonpiezoelectric surfaces and it is planned to use anhydrous alcohol as the coupling fluid for NaCl surface wave excitation. A device is being constructed which allows interdigital electrodes which have been deposited on crystal quartz to be brought into contact with an alcohol film covering portions of the NaCl surface. The electrode separation is variable and the alcohol film thickness can be changed in 2μ steps to study the dispersive properties[3] of this layered transducer configuration. The area of the NaCl sample to be irradiated is not covered by the alcohol film and this area is easily accessible to the 10.6μ beam.

References

(1) M. B. Schulz et. al., J. App. Phys. 41, 2755 (1970).

(2) P. Das, M.N. Araghi, App. Phys. Lett. 16, 293 (1970).

(3) D. Penunuri, K. M. Lakin, IEEE Ultrasonics Symposium, 1972.

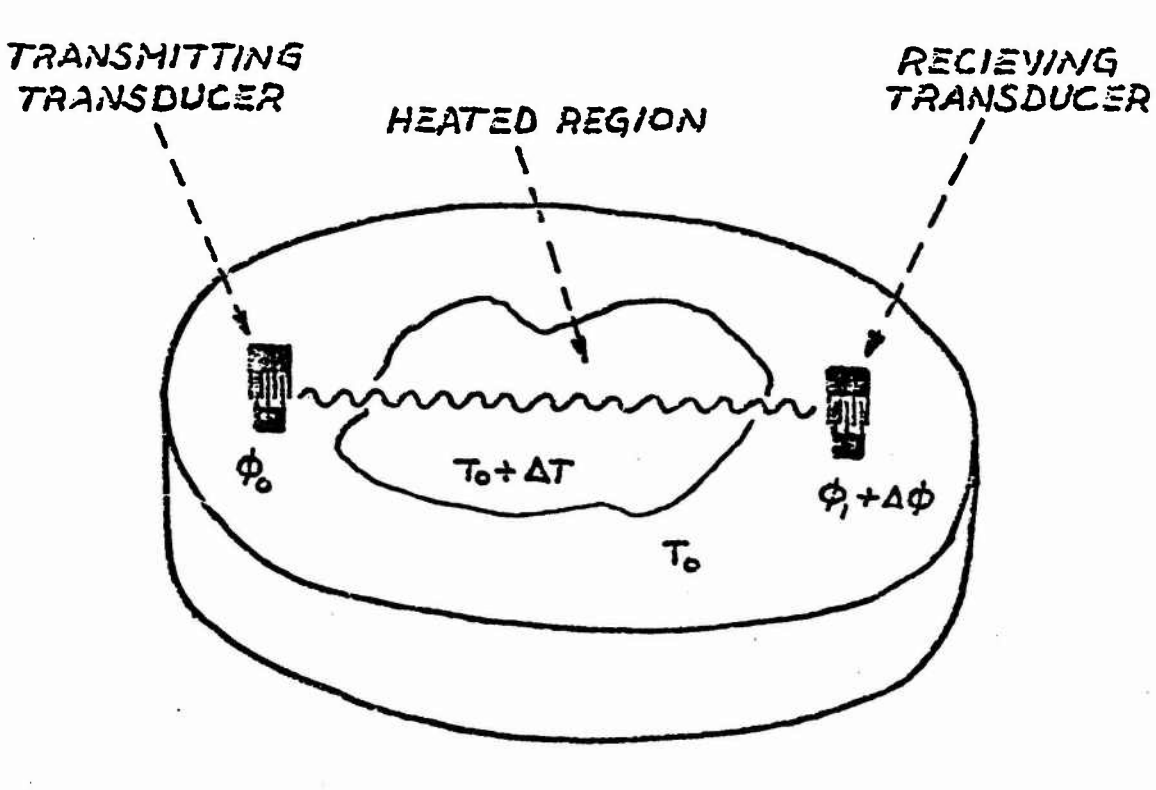

Figure 1

Schematic diagram of acoustic temperature detection depicting the propagation of a surface acoustic wave on a sample surface. The ambient phase difference of an acoustic wave of wavelength λ which has travelled through a transducer separation a is $(\bar{\Phi}_1 - \bar{\Phi}_0) = 2\pi a/\lambda$. The heated region acquires a temperature increase ΔT above the ambient T_0 which induces a phase change $\Delta \bar{\Phi}$ detected at the receiving transducer.

Figure 2

Velocity temperature coefficient for NaCl has been calculated for wave propagation in the XY plane between the [100] and [110] directions. For cubic crystal symmetry this calculation maps the angle variation of α_2 in the entire plane.

FIGURE 2

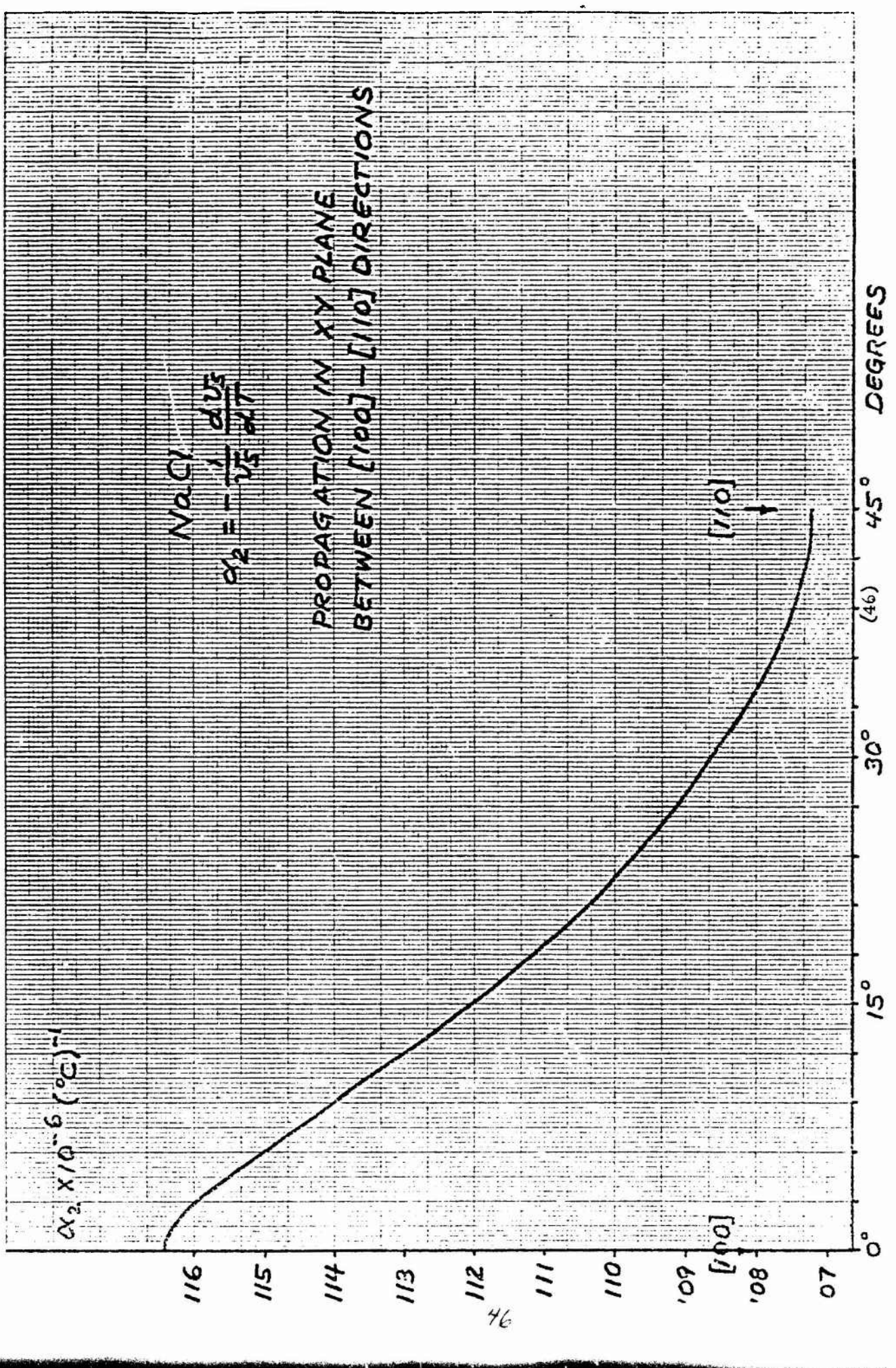
NaCl
$\alpha_2 = -\frac{1}{\sqrt{2}} \frac{d\nu_2}{dT}$
PROPAGATION IN XY PLANE
BETWEEN [100] - [110] DIRECTIONS
$\alpha_2 \times 10^{-6}$ (°C)$^{-1}$
116
115
114
113
112
111
110
109
108
107
[100]
[110]
0°
15°
30°
45°
DEGREES
(46)

Figure 3

Acoustic temperature detection of infrared radiation. This graph indicates the results of a calculation of the steady state phase change $\Delta\Phi$ induced by a temperature increase ΔT. The heating arises from the absorption of 10.6μ infrared radiation by the quartz which has an absorption coefficient $\beta \sim 250 cm^{-1}$. The infrared radiation has a gaussian beam shape spatially and an integrated power of P_o watts. The acoustic wave of wavelength λs and frequency νs propagates through a nonuniformly heated region of length $2S$ on a Y-cut crystal quartz substrate. The transducer separation is 2a.

FIGURE 3

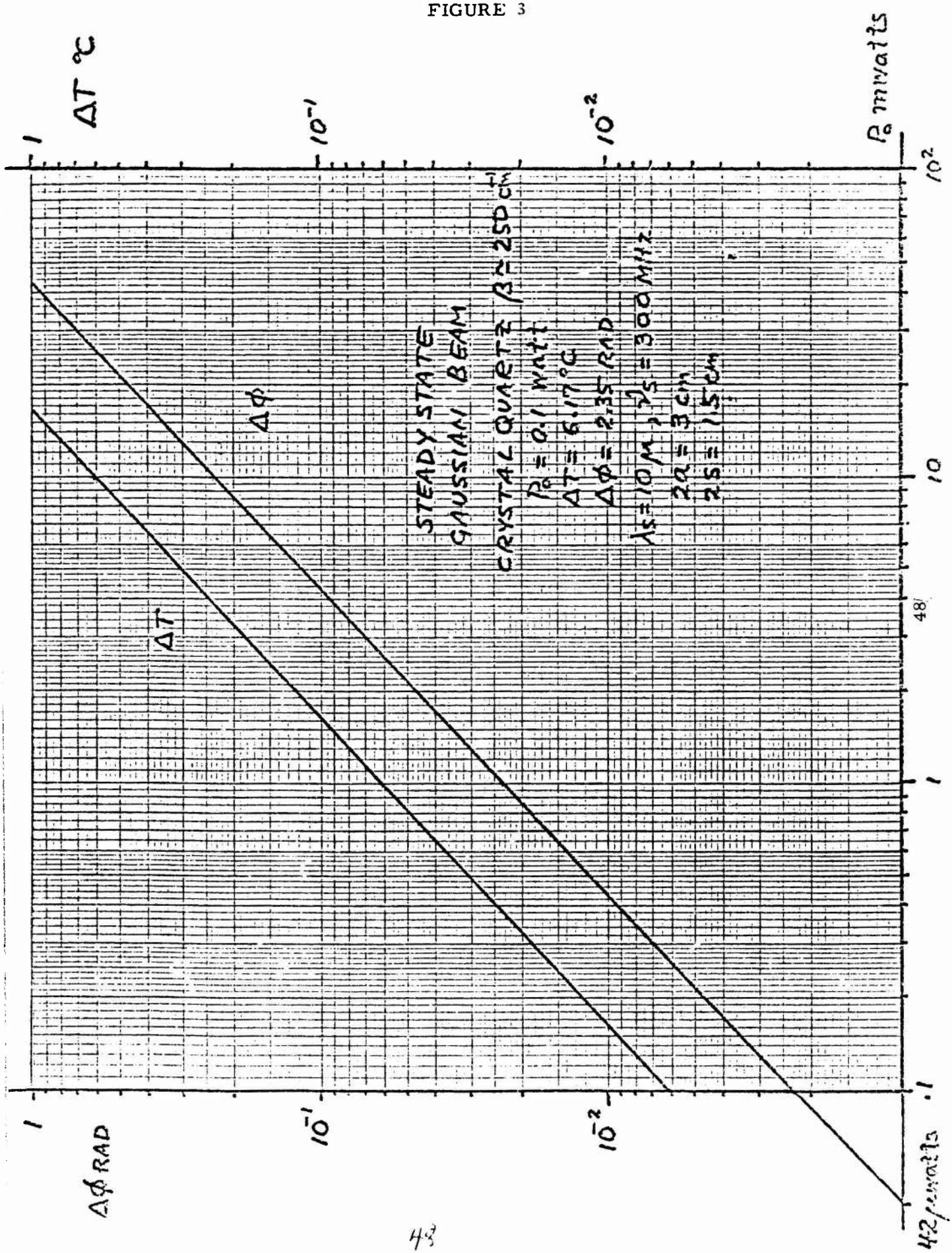
ΔT °C
1
10⁻¹
10⁻²
P₀ milliwatts
10²
STEADY STATE
GAUSSIAN BEAM
CRYSTAL QUARTZ β ≈ 250 cm⁻¹
P₀ = 0.1 watt
ΔT = 6.17°C
Δφ = 2.35 RAD
1s = 10 MILS = 300 MILS
2a = 3 cm
2s = 1.5 cm
Δφ
ΔT
10
1
.1
Δφ RAD
10⁻¹
10⁻²
42 milliwatts

Figure 4

This graph indicates the results of a calculation (similiar to Figure 3) for the steady state phase change induced by 10.6μ radiative absorption in a NaCl sample disk. The acoustic wave propagation is along the [110] direction in the XY plane.

FIGURE 4

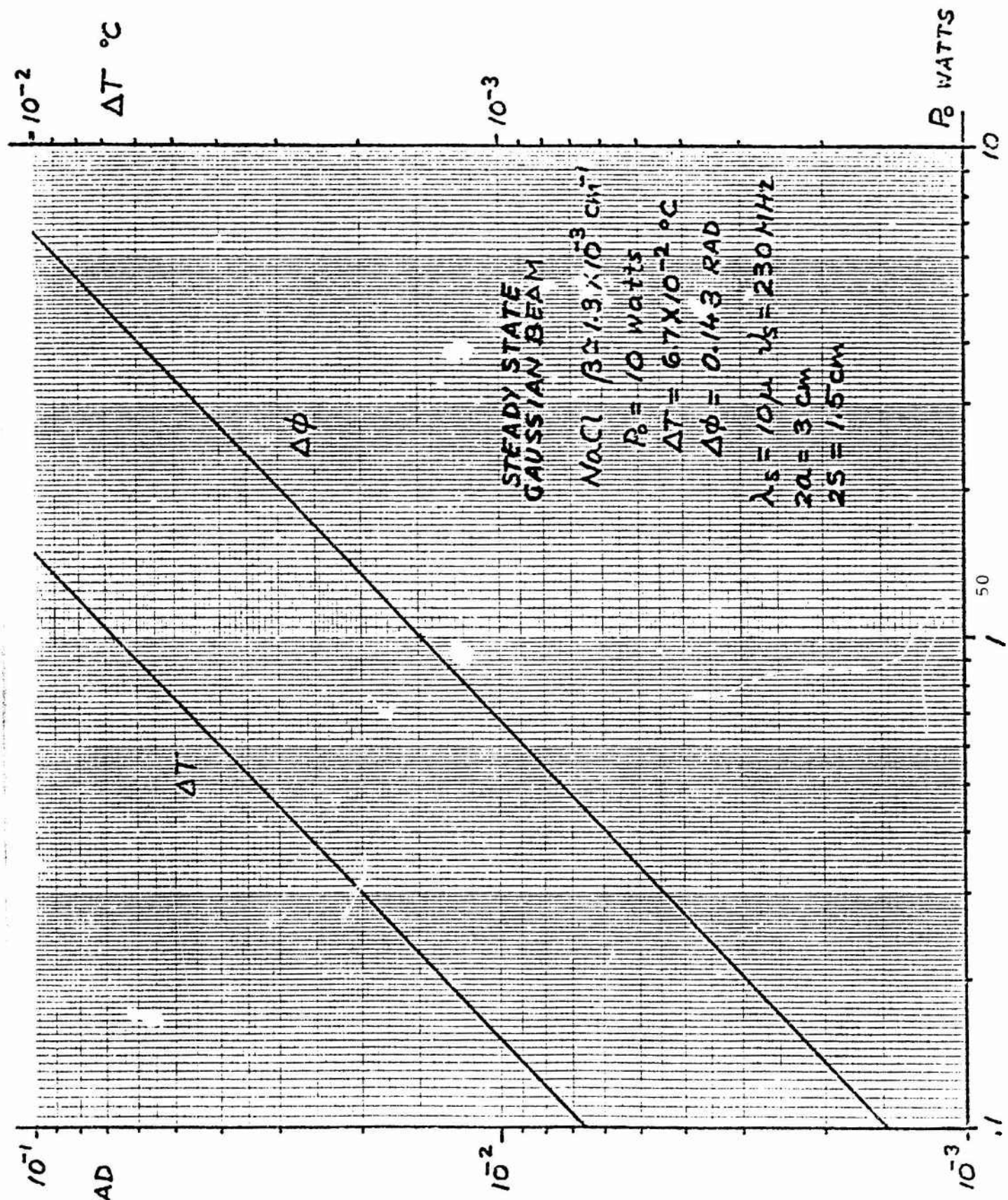
10^{-2}
ΔT °C
10^{-3}
P_0 WATTS
10
1
50
.1
10^{-1}
10^{-2}
10^{-3}
Δφ RAD
Δφ
ΔT
STEADY STATE
GAUSSIAN BEAM
NaCl (β≈1.3×10⁻³ cm⁻¹)
P_0 = 10 watts
ΔT = 6.7×10⁻² °C
Δφ = 0.143 RAD
λ_s = 10μ ν_s = 230 MHz
2a = 3 cm
2s = 1.5 cm

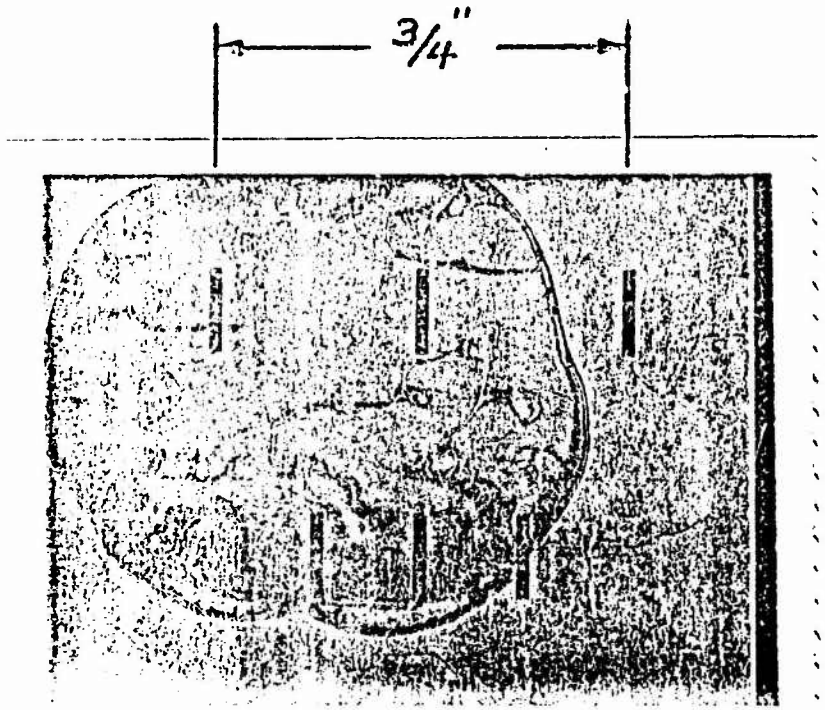

Figure 5 A

This picture shows two sets of interdigital transducers having different transducer separations. Electrode connecting wires have been attached.

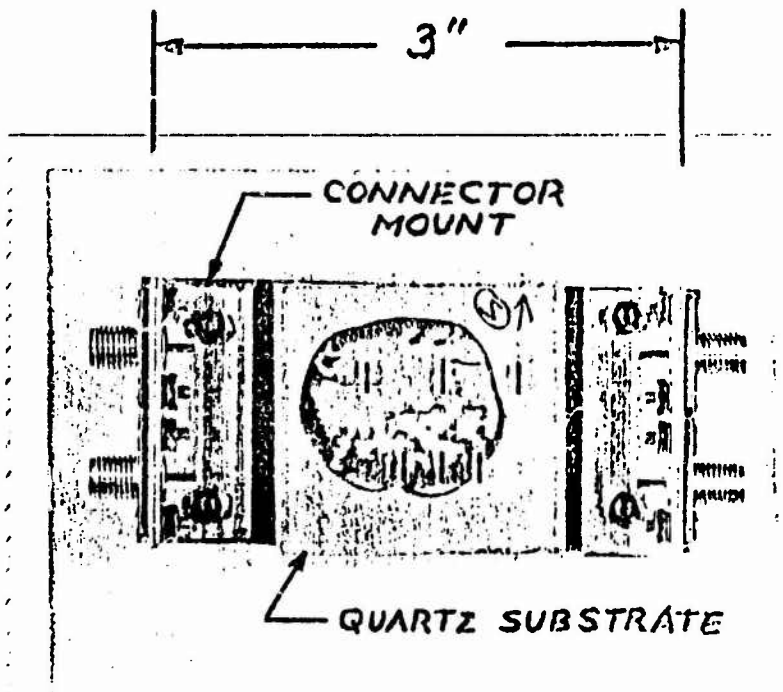

Figure 5 B

This picture shows an assembled acoustic temperature detector constructed with interdigital transducer sets on a Y-cut crystal quartz substrate. The quartz substrate has been bonded (irregular circle) on the bottom surface to an electrode connector mounting.

FIGURE 5

g.1 **Characterization of Optical Performance of IR Window Systems**

John H. Marburger, Martin Flannery

(1) INTRODUCTION.

During this quarter our efforts were concentrated on finding some analytic solutions for stress birefringence in windows with non-axisymmetric temperature profiles. We describe one simple approximation for the stress birefringence in isotropic circular windows with narrow, nearly centered beams, for times short compared to the thermal diffusion time.

(2) NON-AXISYMMETRIC BIREFRINGENCE.

Since small strain thermoelastic theory is linear it obeys the superposition principle, which means that if the temperature distribution is decomposed into a sum of several distributions, the total stress will be the sum of the stresses from each distribution. There are very simple expressions, equations (1), for the stresses in a circular disc due to an axisymmetric temperature profile, $T(r)$:[1]

$$\sigma_{rr} = \alpha E\left[a^{-2}\int_0^a Trdr - r^{-2}\int_0^r Trdr\right] \qquad (1)$$

$$\sigma_{\theta\theta} = \alpha E\left[a^{-2}\int_0^a Trdr + r^{-2}\int_0^r Trdr - T\right]$$

These observations suggest approximating a non-axisymmetric beam by a set of circularly symmetric distributions and finding the stresses from each distribution by solving each problem in a disc centered on the distribution and of the same radius as the window, as illustrated in Figure 1. The total stress is most conveniently found by transforming each stress tensor from polar to Cartesian coordinates, expressing it in terms of the central Cartesian coordinates, and then adding all the tensors. This procedure will avoid the use of complex infinite series usually associated with solutions of non-axisymmetric problems.

Once the stresses are known the indicatrix can be found:

$$B_{ij} = \pi_{ijkl}\,\sigma_{kl} + \left[\frac{1}{n_o^2} + \left(p_{11} + 2p_{12}\right)\alpha T\right]\delta_{ij} \qquad (2)$$

where π is the piezo-optic tensor and p_{11} and p_{12} are the principle elasto-optic coefficients for an isotropic medium. By a suitable transformation the indicatrix can be diagonalized at each point in the window to find the principle axes and refractive indices for the two linearly polarized waves transmitted through the window.

(3) ACCURACY.

For narrow beams centered in large windows we expect the stresses to be quite accurate except near boundaries where they should be $\sigma_{rr}(a) = 0$ and $\sigma_{\theta\theta}(a) =$ constant. These narrow beams will have $T(r > r') \approx 0$ where r' is near the window edge and equations (1) will have the following dependence on r:

$$\sigma_{rr} \propto \left(1 - (a/r)^2\right)$$
$$\sigma_{\theta\theta} \propto \left(1 + (a/r)^2\right) \qquad (3)$$

Thus there's an annulus near the window edge where $\sigma_{rr} \approx 0$ and $\sigma_{\theta\theta} \approx$ constant. This means that slightly off-center temperature distributions will not produce large errors near the edge.

Finally in region B of Figure 1, the expressions from equations (1) for a distribution centered at A are not exactly correct. We can generally ignore that because the intensity and area are small, so the effect on the beam should be small. This problem can be avoided by solving the off-center distributions in discs that are large enough to include the whole window, but this tends to overestimate the stresses in the center where they are important.

In the next quarter we intend to check this approximation against more accurate analytical expressions and to investigate the diffraction of a beam passing through the window.

RFFFRENCFS

1. B. A. Boley and J. H. Weiner, Theory of Thermal Stress, John Wiley and Sons, Inc., New York (1960).

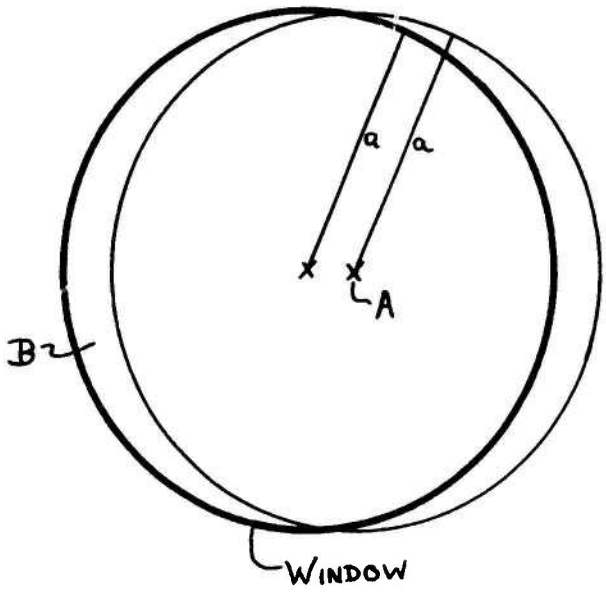

FIGURE 1. Non-axisymmetric Temperature Distribution in a Circular Window.

3. DISCUSSION

Calorimetric absorption measuments (section f.1) performed on additional samples of very pure GaAs indicate that while the absorption coefficient β is slightly lower in samples without Cr compensation, a value significantly lower than .006 cm^{-1} in the 9 to 11 μm region cannot be expected with conventional high temperature melt growth techniques. The limiting absorption mechanism for these samples has not yet been determined, and it is imperative that samples be examined which have been prepared by substantially different growth techniques. We are continuing our efforts to obtain such samples. Temperature dependent calorimetry and IR spectrometry of a variety of samples are now being used to help identify the residual loss mechanism.

Prof. Copley has suggested that bulk window materials can be purified by progressive recrystallization. After (section c.1) was completed, recrystallization was observed in a high purity Cr doped GaAs sample, which had previously been strained. Absorption data has not yet been obtained for the treated sample.

The oxygen pumping concept of J. Whelan (section a.1) has been developed to the point where approximately one monolayer of oxygen can be detected on a cm^2 of GaAs. This technique can be used for detecting or removing trace amounts of oxygen in materials other than GaAs, and promises to be a powerful tool for preparing materials with controlled oxygen content.

Professors Parks and Lakin (section f.2) have developed their acoustical surface wave technique for measuring surface absorption to the point where definite performance characteristics can be estimated. Preliminary experiments have been performed to study the sensitivity and time response of acoustic temperature detection. This technique promises to be an important new way to detect IR radiation by measuring very small temperature changes on the surface of an absorbing sample. Preliminary theoretical studies necessary to extract surface absorption data using this technique for IR window materials have been performed and more extensive studies are planned.

Theoretical work on multiphoton absorption mechanisms is continuing with emphasis on features which are model-independent. Prof. Hellwarth and coworkers have discovered a class of sum rules for the frequency moments of the absorption coefficient which will allow various approximate techniques to be assessed. Work in this field is plagued by the necessity to invoke sweeping approximations to simplify the analysis. If theory is ever to be of practical value in estimating absorption magnitudes in the absence of definitive experiments, it is necessary to construct a credible system of theoretical checks to test the accuracy of the prediction. Our work is strongly influenced by this philosophy.

Our efforts to understand the large thermal beam slewing effect observed by Skolnik of AFCRL are continuing. The material reported in (section g.1) is the result of an effort to include stress induced birefringence effect in the theory for acentric beam transmission. This problem is complicated by the lack of symmetry, but we will soon be able to estimate the contribution of this effect.

The ultra pure alkali halide production facility is now in full operation. Material is being tested here for low temperature absorption spectra and calorimetry. If the results of these test are satisfactory, specimens will be sent to other AF contractors for preparation of polycrystalline samples.

During this quarter, we profited from visits by A. Kahan, B. Bendow, and L. Skolnik (AFCRL) and M. Stickley (ARPA). In connection with our regular weekly IR Window Seminar for all USC contract participants, we also received visits from H. Bennet and colleagues from the Naval Weapons Center, and representatives from other contractors in the field including Oklahoma University and North American Rockwell.

4. SUMMARY

The method described previously for measuring and controlling minute quantities of oxygen impurities has been used to remove oxygen prior to and during the growth of epitaxial GaAs at 600°C. The detection limit of the technique is about one monolayer of oxygen on a cm^2 of GaAs.

Ultra pure KCℓ has been prepared by the process described in previous reports. The apparatus produces several gallons of purified KCℓ solution per day. Single crystals of this material have been pulled from the melt, but have not been fully analyzed at the time of this report.

Progress is being made on the chemical vapor growth of GaAs. Progressive refinements of the open tube growth facility have produced samples of progressively higher quality. So far no samples have been produced of sufficient thickness for absorption measurements.

Further measurements of the mechanical properties of GaAs have been made. We suggest that relatively low temperature purification of semiconductor materials may be accomplished by recrystallization of strained samples.

The defect state of CdTe at elevated temperatures is still under investigation. Results during this quarter deal with higher dopant levels of In, self diffusion effects in nonstoichiometric samples, and related phenomena.

A class of sum rules for the frequency moments of the multiphonon absorption coefficient have been discovered. These have been used to show that commonly omitted terms in the approximate analysis of multiphonon absorption are definitely comparable to the terms retained.

Tunable calorimetry has been employed to characterize high purity samples of GaAs. These measurements indicate that a lower limit of absorption in the 10.6μm region has been reached for high temperature melt grown samples. We conclude that it is imperative to examine samples prepared under more widely differing conditions. The lowest absorbances measured to date have been in samples which were not compensated with Cr.

An extensive report on the acoustical surface wave technique for optical absorption measurements is included. Preliminary experiments indicate that the technique can detect millidegree temperature changes in surface layers from 0.1 to 100 microns in depth. The technique also promises to be valuable for infrared detection.

Numerical simulation of beam slewing in windows heated by acentric beams is being extended to include the effects of induced birefringence. The problem is difficult because of the lack of circular symmetry, but important because simulation which omits induced birefringence fails to account for the observed beam slew magnitude for a KCℓ window. During this period an approximate formulation of acentric stress birefringence was developed.